DANIEL MARGERIT AND DWIGHT BARKLEY

Singular perturbation equations for 3-d excitable media

In this paper the idea of Prandtl's boundary layer is exported to a field other than fluid dynamics. Excitable media, such as nerve fibers and heart tissue, are typically modelled with reaction-diffusion equations containing two chemical species that evolve on very different time scales. In three dimensions solutions of these equations take the form of rotating scroll waves (interfaces) ending on filaments. The ratio of the two times scale defines a natural small parameter epsilon. Exploiting the inherent smallness of epsilon, singular perturbation methods are used to derive three-dimensional equations for each of two boundary layers : interface region (scroll) and filament region (core), and for the associated outer region. For scrolls with uniform twist about straight filaments, this matched asymptotic expansion method is also used to derive free-boundary equations not only at leading order but also at first order. Both orders are validated against full solutions of the reaction-diffusion equations. Using these two orders and with no adjustable parameters, the shape and frequency of waves are correctly predicted for most cases of physical interest.

1. Introduction

In three-dimensional excitable media, propagating waves of excitation typically take the form of scrolls which are organized about one-dimensional filaments[13]. These filaments have some similarities to the vortex filaments found in fluid dynamics. However, unlike vortex filaments in fluid dynamics, filaments in excitable media can have associated *twist.* Figure 1 illustrates this by showing a scroll wave which is uniformly twisted along a straight filament. The purpose of this paper is to show how the idea of Prandtl's boundary layer can be applied to excitable media. In particular we derive equations predicting the shape and rotation frequency of scroll waves such as in Fig. 1 and through these equations we are able to understand and predict the role of twist in shape and frequency selection.

We begin by considering the following partial-differential-equation (PDE) model of excitable media[1] written in the space-time scales proposed by Fife[6]:

$$\epsilon^2 \partial u/\partial t = \epsilon^2 \nabla^2 u + u\,(1-u)\left(u - \frac{v+b}{a}\right), \tag{1}$$

$$\partial v/\partial t = \epsilon(u-v). \tag{2}$$

Such two-component reaction-diffusion models capture essential properties of excitable media and are widely used in theoretical and computational studies, e.g. [2, 3, 7, 8, 9, 14]. Model parameters a and b control the excitation threshold and duration and will have values $a = 0.8$ and $b = 0.1$ throughout. The parameter ϵ is small, reflecting the disparate time scales of the fast activator variable u and slow inhibitor variable v.

Previous work on wave selection in excitable media through asymptotic expansions [3, 7, 8, 9, 12] has focused entirely on leading order in the small parameter ϵ and primarily on two dimensions. Expanding the rotation frequency as

$$\omega = \omega^{(0)} + \epsilon\omega^{(1)} + \ldots, \tag{3}$$

only the leading-order frequency $\omega^{(0)}$ has been obtained[3, 7]. While the small-ϵ (Fife) limit has played an important role in 2D studies, the leading order does not accurately predict many properties of waves at finite ϵ. However, we find (Fig. 3 below) that expansions to *first order* in ϵ are predictive well into regimes of physical interest.

2. Geometry, asymptotic description and leading order solution

For the leading-order asymptotics, we begin by considering the general three-dimensional (3D) case. The medium is divided into three regions: outer, interface, and core as shown in Fig. 2. The filament is the curve $\mathbf{X}(s,t)$ inside the core. The outer region comprises the bulk of the medium. It consists of both excited (+) and quiescent (-) portions for which $u = u^+ = 1$ and $u = u^- = 0$, respectively, to all orders in ϵ. Expansion of the v-field in the outer region gives: $v = v^s + \epsilon v^{(1)} + \ldots$, where $v^s = -b + a/2$ is the stall concentration (value such that a plane interface is stationary) and $v^{(1)}$ is to be determined.

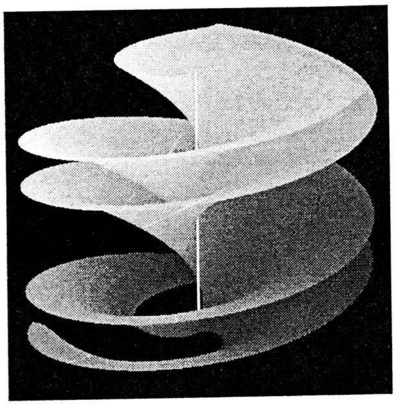

Figure 1: Twisted scroll wave from numerical solutions of Eqs. (1-2). Isosurface is shown for $u = 0.5$. The filament is white. The structure rotates in time with frequency ω about the filament. The twist is $\tilde{\tau} = 0.5$, (defined later in the text); $\epsilon = 0.1$.

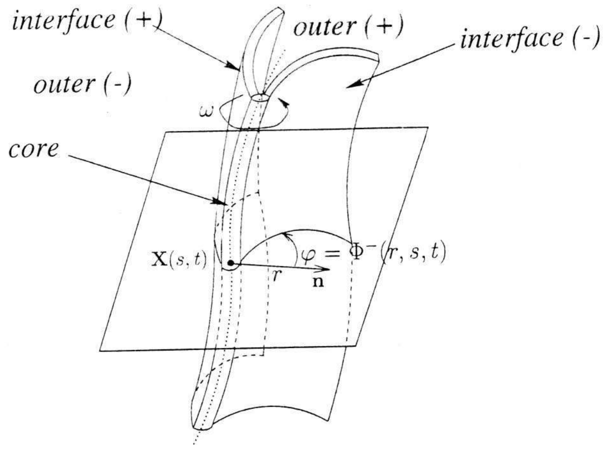

Figure 2: Scroll geometry showing outer regions [excited (+) and quiescent (-)], interface regions [wavefront (+) and waveback (-)], and core region. The filament $\mathbf{X}(s,t)$ is parameterized by s and time t. Local coordinates to the filament are (r,φ,s), with (r,φ) in the plane normal to $\mathbf{X}(s,t)$ and φ measured from the normal vector $\mathbf{n}$.

Separating excited and quiescent states are the thin interfaces where u undergoes rapid change. These consist of a wave front (+) and a wave back (-), which on the outer scale are given by $\varphi = \Phi^{\pm}(r,s,t)$. Solving leading- and first-order inner equations for u across the interface (v is constant at these orders across the interface) and matching to the outer u-solution, one obtains equations for interface motion[10]. Thus Eqs. (1-2) reduce to equations for $v^{(1)}$ in the outer region together with equations for the motion of the two interfaces (free boundaries):

$$\partial v^{(1)}/\partial t = u^{\pm} - v^{s}, \tag{4}$$

$$-\frac{r\dot{\Phi}^{(0)\pm}h^{\pm}}{\sqrt{m^{\pm}}} = 2H^{\pm} \pm \frac{\sqrt{2}}{a}v^{(1)\pm} \tag{5}$$

where $\Phi^{(0)\pm}$ is the leading order approximation to $\Phi^{\pm}$, and where $h^{\pm} \equiv |\partial\mathbf{X}/\partial s|\,(1 - rK\cos\Phi^{(0)\pm})$, K is the filament curvature, $m^{\pm}$ is the determinant of the metric tensor and $H^{\pm}$ is the mean curvature of interface $\Phi^{(0)\pm}$, and finally $v^{(1)\pm}$ is the value of $v^{(1)}$ at interface $\Phi^{(0)\pm}$. Eq. (5) equates normal velocity of the interface to twice the mean curvature plus the speed of a plane interface. Phenomenological approaches to excitable media yield similar equations [16]. As in 2D [9], the core plays no role at leading order other than to regularize the cusp that would otherwise exist as the two interfaces come together. However, leading-order core equations dictate that $\dot{\mathbf{X}}^{(0)} = 0$, i.e. the filament velocity is zero at leading order in ϵ and filament motion must come at higher order.

We now consider the specific case of a straight filament and seek solutions with uniform twist $\tau \equiv \partial\Phi/\partial s$ and constant frequency $\omega^{(0)} = \dot{\Phi}^{(0)}$. The angle between the two interfaces can be shown to be constant: $\Delta\Phi^{(0)} = \Phi^{(0)-} - \Phi^{(0)+} = 2\pi(1-v^{s})$ and $v^{(1)\pm}$ can be eliminated from the free-boundary equations to obtain a single equation describing the shape of the interface[10]:

$$q\frac{d\Psi^{(0)}}{d\tilde{r}} + \frac{\Psi^{(0)}(1+\Psi^{(0)^2})}{\tilde{r}} = \tilde{r}(q+\Psi^{(0)^2}) - B(q+\Psi^{(0)^2})^{3/2}, \tag{6}$$

where $\Psi^{(0)} \equiv rd\Phi^{(0)+}/dr = rd\Phi^{(0)-}/dr$, and $q \equiv 1+\tilde{\tau}^2\tilde{r}^2$, with $\tilde{r} = \sqrt{\omega^{(0)}}r$, $\tilde{\tau} = \tau/\sqrt{\omega^{(0)}}$. The eigenvalue B is related to $\omega^{(0)}$ and model parameters via $B = (\mu/\omega^{(0)})^{3/2}$ where $\mu^{3/2} = \sqrt{2}\pi v^{s}(1-v^{s})/a$. With $\tilde{\tau} = 0$ (2D case), Eq. (6) is as given by Karma[7], while for $\tilde{\tau} \neq 0$ it can be shown to agree with the work of Bernoff [3]. $\Psi^{(0)}$ and the selected B as a function of $\tilde{\tau}^2$ is found[11] from Eq. (6) by shooting: integrating from $\tilde{r} = 0$ to large $\tilde{r}$ and finding B such that $\Psi^{(0)}$ matches the relevant large-r limit obtained from Eq. (6).

3. Order-ϵ asymptotic for a straight filament with twist

We now consider the order-ϵ asymptotics. We treat only the case of straight filaments. For scrolls with twist τ rotating at frequency ω: $\partial/\partial t = -\omega\partial/\partial\varphi$ and $\partial/\partial z = \tau\partial/\partial\varphi$. For this case Eqs. (1-2) become

$$\epsilon^2\omega\partial u/\partial\varphi \quad + \quad \epsilon^2\nabla_\perp^2 u + u\,(1-u)\left(u - \frac{v+b}{a}\right) = 0, \tag{7}$$

$$\omega\partial v/\partial\varphi \quad + \quad \epsilon(u-v) = 0, \tag{8}$$

where $\nabla_\perp^2 = \partial^2/\partial r^2 + (1/r)\partial/\partial r + (q/r^2)\partial^2/\partial\varphi^2$. The major complication in deriving free-boundary equations from Eqs. (7-8) is matching outer and inner solutions (for u and v) across the interface because $v^{(2)}$ is not constant across the interface and because the normal to the interface lies outside the (r,φ) plane when $\tau \neq 0$. For this we use local coordinates "normal" to $\nabla_\perp^2$ near the interface[10].

The symbolic calculator Maple is used to obtain the cascade of asymptotic equations in both the outer and inner regions up to the order of interest. The outer asymptotic expansion is plugged into Eqs. (7-8). For the inner region, Maple is first used to express Eqs. (7-8) in local inner coordinates in the interface region and then used to plug the inner asymptotic expansions into these equations. Maple is then used to find the behavior at infinity of the inner solution and to perform the intricate asymptotic matching with the outer solution. Finally, Maple is used to find the asymptotic behavior at infinity of $\Psi^{(0)}$ and $\Psi^{(1)}$ to many orders in $\tilde{r}$. The symbolic calculator allows us to quickly derive these results and to minimise the possibility of mistakes in such fastidious calculus.

The result is that at this order $\Delta\Phi^{(1)} = \Phi^{(1)-} - \Phi^{(1)+} = 0$ and it is again possible to obtain a single equation for $\Psi^{(1)} \equiv a\omega^{(0)} r d\Phi^{(1)\pm}/dr$[11] with an eigenvalue D related to $\omega^{(1)}$ by $D = a\omega^{(1)}$. The general solution of this equation is found[11] and diverge exponentially at infinity unless D has a selected value.

Finally, we use symbolic calculation to verify that the fields obtained asymptotically is truly the solution of Eqs. (7-8) up to the order of interest. This is an exact check which is independent of the calculus used to derived the asymptotic fields. We perform this verification with Maple by (i) plugging into Eqs. (7-8) the outer asymptotic solution and equations for $\Psi^{(0)}$ and $\Psi^{(1)}$ up to the relevant order, then expanding in ϵ and verifying that $0 = 0$ on the computer; (ii) doing the same for the inner asymptotic solution and with Eqs. (7-8) written in the local stretched coordinates (but not expanded in ϵ); (iii) checking the matching between the outer and inner asymptotic solutions. Such a check is important in boundary layer problems. The symbolic calculator makes this check easy to perform and thus provides a strong and useful tool for singular perturbation calculus.

4. Comparison with the numerical PDE solution and conclusion

We now compare the asymptotic results with full PDE solutions. For this we solve (7-8) using Newton's method [2]. The operator $\nabla_\perp^2$ is discretized on a polar grid typically with 256 points in φ and radial spacing $\Delta r = 0.05$. The r-derivatives are computed by finite differences and φ-derivatives are computed spectrally.

Figure 3 shows the dependence of ω on ϵ from the PDE solutions. This figure clearly shows the existence of the Fife limit: a finite-frequency limit as $\epsilon \to 0$. Over a substantial range of ϵ, the frequency is very well captured by the first two orders in ϵ: $\omega \simeq \omega^{(0)} + \epsilon\omega^{(1)}$. Extrapolation of frequency data to $\epsilon = 0$ gives $\omega^{(0)}$ and thus B. The slope of ω versus ϵ gives $\omega^{(1)}$ and hence D. From the computed u-fields we find the functions $\Phi^{\pm}$ as curves on which $u = 1/2$ and from these Ψ is computed by differencing. Analogously to the frequency, from the dependence of Ψ on ϵ we find $\Psi^{(0)}$ and $\Psi^{(1)}$[11]. The core radius is found to be $r \simeq 8\epsilon$ and the data also confirm that $\Delta\Phi^{(1)} = 0$.

In Fig. 4 we compare full solution of the stationary PDE (7-8) with the interface curves. Shown is a cross-section of a twisted scroll wave normal to the straight filament $\mathbf{X}$ at station s and instant t in the domain, $r \leq 20$. Also shown is cross-section of the stationary interface at leading-order $\varphi = \Phi^{(0)\pm}(r,s,t)$ and at leading-plus-first-order $\varphi = \Phi^{(0)\pm}(r,s,t) + \epsilon\Phi^{(1)\pm}(r,s,t)$. Figures 4(b) and (d) show the same case as Fig. 1 (apart from the domain radius). The agreement is excellent and contains no adjustable parameters.

In conclusion, we have derived free-boundary equations at leading-order and first-order for twisted scroll waves in excitable media and we have validated these equations directly with numerical solutions of the underlying PDEs. The free-boundary equations we have derived apply to a large class of models [10]. For excitable media it would be of considerable interest to derive an equation of motion for this filament as has been successfully performed in hydrodynamics for vortex filaments[4].

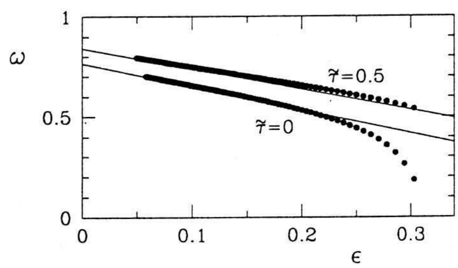

Figure 3: Scroll frequency ω versus ϵ from numerical solutions of the PDE model for two values of twist. Lines are from fits to the data at small ϵ and are indistinguishable from asymptotic predictions at first order in ϵ.

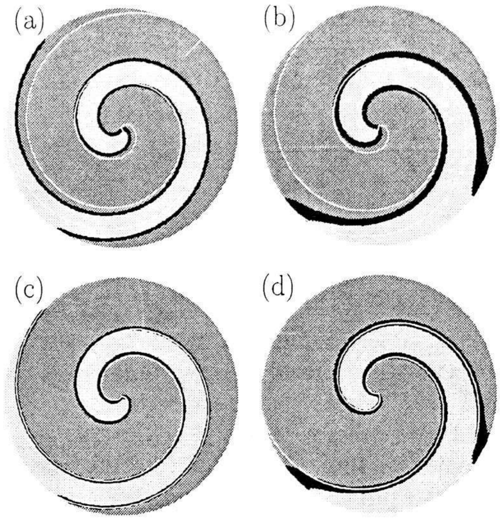

Figure 4: Comparison between PDE solutions (greyscale) and asymptotic results (white curves). (a) $\tilde{\tau} = 0$, asymptotics at leading order. (b) $\tilde{\tau} = 0.5$, asymptotics at leading order. (c) $\tilde{\tau} = 0$, asymptotics at leading-plus-first order. (d) $\tilde{\tau} = 0.5$, asymptotics at leading-plus-first order. Black is the interface $0.1 \leq u \leq 0.9$; light grey (dark grey) is $u < 0.1$ ($u > 0.9$). The radius is 20; $a = 0.8$, $b = 0.1$, $\epsilon = 0.1$.

5. References

1 Barkley, D.: A model for fast computer simulation of waves in excitable media; Physica D **49** (1991), 61–70.

2 Barkley, D.: Linear Stability Analysis of Rotating Spiral Waves in Excitable Media; Physical Review Letters **68** No. 13 (1992), 2090–2093.

3 Bernoff, A.J.: Spiral wave solutions for reaction-diffusion equations in a fast reaction/slow diffusion limit; Physica D **53**(1991), 125–150.

4 Callegari, A.J., Ting, L.: Motion of a curved vortex filament with decaying vortical core and axial velocity; SIAM J. Appl. Math. **35** No. 1, (1978), 148-175

5 Fenton, F., Karma, A.: Vortex dynamics in 3 dimensional continuous myocardium with fiber rotation : filament instability and fibrillation; Chaos **8** No. 1 (1998), 20–47.

6 Fife, P.C.: Understanding the Patterns in the BZ Reagent; Journ. of Statistical Physics **39** No. 5/6 (1985), 687–703.

7 Karma, A.: Scaling Regime of Spiral Wave Propagation in Single-Diffusive Media; Physical Review Letters **68** No. 3 (1992), 397–400.

8 Keener, J.P., Tyson, J.J.: The Dynamics of Scroll Waves in Excitable Media; SIAM Review **34** No. 1 (1992), 1–39.

9 Kessler, D.A., Levine, H., Reynolds, W.: Theory of the spiral core in excitable media; Physica D **70** (1994), 115–139.

10 Margerit, D., Barkley, D.: to be published (2000).

11 Margerit, D., Barkley, D.: Selection of twisted scroll waves in three-dimensional excitable media; to appear in Phys. Review Letters (2000).

12 Mikhailov, A.S., Zykov, V.S.: Kinematical theory of spiral waves in excitable media: Comparison with numerical simulations; Physica D **52** (1991), 379–397.

13 Winfree, A.T.: Stable Particle-Like Solutions to the Nonlinear Wave Equations of Three-Dimensional Excitable Media; SIAM Review **32** No. 1 (1990), 1–53.

14 Winfree, A.T.: Varieties of spiral wave behavior: An experimentalist's approach to the theory of excitable media; Chaos **1** (1991), 303-334.

15 Winfree, A.T.: Persistent tangles of vortex rings in excitable media; Physica D **84** No. 1-2 (1995), 126–147.

16 Yamada, H., Nozaki, K.: Dynamics of untwisted scroll rings in excitable media; Journal of the physical society of Japan **63** No. 2 (1994), 379–382.

Addresses: Dr. Daniel Margerit, Dr. Dwight Barkley, Mathematics Institute, University of Warwick, Coventry CV4 7AL, UK